Comprehensive Comparison of Switching Models for Perpendicular Spin-Transfer Torque MRAM Cells

Simone Fiorentini
Christian Doppler Laboratory for Magnetoresistive Nonvolatile Memory and Logic
Institute for Microelectronics, TU Wien
Vienna, Austria
fiorentini@iue.tuwien.ac.at

Roberto Orio
Christian Doppler Laboratory for Magnetoresistive Nonvolatile Memory and Logic
Institute for Microelectronics, TU Wien
Vienna, Austria
orio@iue.tuwien.ac.at

Wolfgang Goes
Silvaco Europe Ltd
Cambridge, United Kingdom
wolfgang.goes@silvaco.com

Johannes Ender
Christian Doppler Laboratory for Magnetoresistive Nonvolatile Memory and Logic
Institute for Microelectronics, TU Wien
Vienna, Austria
ender@iue.tuwien.ac.at

Viktor Sverdlov
Christian Doppler Laboratory for Magnetoresistive Nonvolatile Memory and Logic
Institute for Microelectronics, TU Wien
Vienna, Austria
sverdlov@iue.tuwien.ac.at

***Abstract*—Simulations of free-layer switching in spin - transfer torque MRAM are usually performed with the torque computed approximately by assuming a position-independent electric current density through the structure. For high values of the tunneling magnetoresistance, this description is not accurate anymore, and one needs to solve the spin and charge drift-diffusion equations in the whole structure self-consistently. We compute the switching time distribution obtained by the self-consistent model and compare it to the switching times from the fixed current density approach. We show that, provided the current is appropriately adjusted, the simplified model can mimic the correct switching time distribution even in the case of high TMR.**

Keywords—Spin-transfer torque, MRAM, perpendicular magnetization, tunneling magnetoresistance

I. Introduction

In recent years, the development of computer memory has been focused on miniaturization and scaling of semiconductor devices. This, however, has increased the stand-by power and leakages in modern integrated circuits, due to the volatile nature of SRAM and DRAM. An attractive path to dramatically reduce the power consumption is to introduce non-volatility.

One possible path to achieve this goal is to consider the spin degree of freedom of electric charges. For this, non-volatile spin-transfer torque (STT) magnetoresistive random access memory (MRAM) is a viable candidate. STT-MRAM combines higher speed, superior endurance and lower costs as compared to flash memories. In addition, STT-MRAM is compatible with CMOS technology and can be straightforwardly embedded in circuits. The potential market for STT-MRAM is ranging from IoT and automotive applications to embedded DRAM and L3 caches [1][2].

In this work we present a way of computing the magnetization dynamics in a STT-MRAM by solving the spin drift-diffusion equations with non-uniform current density, and compare it to the standard approach which prescribes the current density to be fixed and position-independent.

II. STT-MRAM

The key element of modern MRAM cells consists of a magnetic tunnel junction (MTJ), formed by two ferromagnetic layers separated by a thin oxide layer, where the latter provides the tunnel barrier (see Fig. 1 for reference). The magnetization of the layers has two possible configurations: parallel (P) and anti-parallel (AP). The magnetization in one of the layers is free to switch (free layer), while the magnetization in the second is fixed (reference layer). This can be achieved by tuning the geometry of the layers or by antiferromagnetically coupling it to a pinned layer [3].

Due to the tunneling magnetoresistance effect, tunneling electrons polarized by the reference layer are easily accommodated by the free layer when the magnetization vectors of the layers are parallel, so the resistance R_P is lower than the resistance R_{AP}. This resistance difference is usually characterized by the tunneling magnetoresistance ratio (TMR), defined as

$$TMR = \frac{R_{AP} - R_P}{R_P}. \qquad (1)$$

Achieving a high TMR ratio is important in order to reliably discern between the P and AP configurations. The use of a CoFeB/MgO/CoFeB MTJ can grant a TMR ratio of up to 600% [4].

The commercial application of MRAM in embedded circuits requires a reliable switching process between the two magnetization configurations of the MTJ. Such a switch can be efficiently realized by letting an electric current flow through the structure: the spins of the electrons get polarized by the reference layer, and the exchange coupling with the magnetization provides the torque (STT) necessary to rotate

978-1-7281-0940-4/19/$31.00 ©2019 IEEE

the magnetization in the free layer and achieve switching [5][6].

In order to design more efficient memories, it is necessary to introduce methods of simulating the switching process in realistic structures.

III. Models

The equation that describes magnetization dynamics is the Landau-Lifshitz-Gilbert (LLG) equation. When introducing a term describing STT ($\mathbf{T_S}$), the final magnetization equation is [7]

$$\frac{\partial \mathbf{m}}{\partial t} = -\gamma \mathbf{m}\times\mathbf{H}_{\text{eff}} + \alpha \mathbf{m}\times\frac{\partial \mathbf{m}}{\partial t} + \frac{1}{M_S}\mathbf{T_S}$$

$$\mathbf{T_S} = \gamma\frac{\hbar}{2e}\frac{0.5\,Jc\,P}{d\left(1+P^2\cos\theta\right)}\mathbf{m}\times(\mathbf{m}\times\mathbf{x}), \qquad (2)$$

where $\mathbf{m}=\mathbf{M}/M_S$ is the position-dependent normalized magnetization in the free layer, M_S is the saturation magnetization, α is the Gilbert damping constant, γ is the gyromagnetic ratio, $\hbar$ is the reduced Plank constant, e is the electron charge, J_C is the current density, P is the spin current polarizing factor [8] assumed to be equal in both ferromagnetic layers, d is the thickness of the free ferromagnetic layer, θ is the angle between local magnetization vectors in the free and fixed layer, and $\mathbf{x}$ is the unit vector along the fixed layer magnetization (Fig. 1). The effective magnetic field $\mathbf{H}_{\text{eff}}$ includes the external field, the magnetic anisotropy field, the demagnetizing field and the stray field from the reference layer/magnetic stack. It also includes the thermal field, a randomly fluctuating magnetic field used to simulate the effects of finite temperature on the magnetization dynamics.

The usual approach in micromagnetic simulations of STT switching is to assume that the current density J_C is position-independent [9]. For low TMR and in-plane MTJs, where the resistance difference between the low and high resistance configuration is small, this assumption can be justified [10]. However, modern MTJs are perpendicularly magnetized (p-MTJs) and possess a large TMR above 200%. In this case the simplified description offered by (2) may not be accurate anymore. Indeed, if the current is running, the local magnetization vectors at every point are not collinear. This results in position-dependent current density, which in turn results in position-dependent spin currents and spin torques at every time step. The validity of (2) must be justified by a complete computation of spin accumulation and spin torques in p-MTJs due to the position dependent current density coupled to the magnetization dynamics.

In order to achieve this, we need to take into consideration the spin and charge drift-diffusion equations [11][12]:

$$\mathbf{J_S} = \frac{\mu_B}{e}\beta_\sigma\sigma\left(\mathbf{J_C} + \beta_D D_e \frac{e}{\mu_B}[(\nabla\mathbf{S})\mathbf{m}]\right)\otimes\mathbf{m} - D_e\nabla\mathbf{S} \qquad (3)$$

$$\frac{\partial \mathbf{S}}{\partial t} = -\nabla\mathbf{J_S} - D_e\left(\frac{\mathbf{S}}{\lambda_{sf}^2} + \frac{\mathbf{S}\times\mathbf{m}}{\lambda_J^2} + \frac{\mathbf{m}\times(\mathbf{S}\times\mathbf{m})}{\lambda_\varphi^2}\right), \qquad (4)$$

where $\mathbf{J_S}$ is the spin current density, μ_B is the Bohr magneton, β_σ and β_D are polarization parameters, σ is the electron conductivity, D_e is the electron diffusivity constant, λ_{sf}, λ_J, λ_φ are scattering lengths, and $\otimes$ stands for the tensor product.

We compute the electric current density $\mathbf{J_C}$ by taking into consideration the dependence of the tunnel barrier resistance on the relative angle of magnetization vectors in the reference and free layer. In order to do this, we solve the Laplace equation $-\nabla^2 V = 0$, where V is the electric potential, in the ferromagnetic contacts. The non-uniform resistance of the barrier, described as [10]

$$R(\theta) = R_P\left(1+\left(\frac{\text{TMR}}{2}\right)\cdot(1-\cos(\theta))\right), \qquad (5)$$

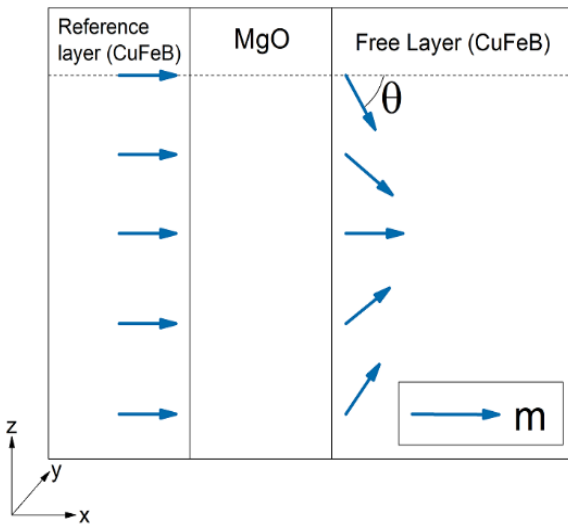

Fig. 1. Schema of the magnetization configuration in a mid-switch scenario.

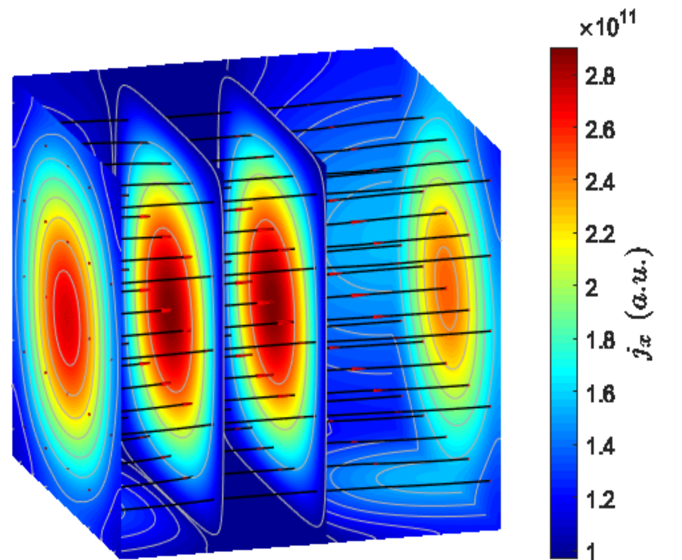

Fig. 2. Current density distribution through a square MTJ in a mid-switch scenario. The current flow is higher where the magnetization is aligned, due to lower resistance.

is imposed by Neumann boundary conditions at the interface between the ferromagnetic and the oxide layers. Dirichlet boundary conditions are imposed on the electrodes, thus fixing the potential. The current density $\mathbf{J_C}$ across the structure is then given by

$$\mathbf{J_C} = -\sigma\nabla V. \quad (6)$$

In Fig. 2 we report the computed current density for the magnetization configuration schematized in Fig. 1. The current density is highly nonhomogeneous and redistributed in order to accommodate the varying resistance across the barrier.

With $\mathbf{J_C}$ known, (3) and (4) can be solved to compute the spin accumulation **S.** The torque term to be inserted in the LLG equation is thus:

$$\mathbf{T_S} = -\frac{D_e}{\lambda_J^2}\mathbf{m}\times\mathbf{S} - \frac{D_e}{\lambda_\varphi^2}\mathbf{m}\times(\mathbf{m}\times\mathbf{S}). \quad (7)$$

IV. Results

We compare the model described by (3-7) (Model 1) with a *fixed voltage* across the MTJ, to the model with the *constant current* density described by (2) (Model 2) and to a reference model [10] generalized to p-MTJs, in which the total *current* is fixed but redistributed at every time step according to the local resistance value (Model 3). In order to account for the differences between the models, we set the total currents for Model 2 and Model 3 to the value of the current in Model 1 at the beginning of the switching process. The simulations are performed for a p-MTJ. The system's main parameters, which were set to typical experimental values [13], are summarized in Table 1. The stack is of a circular pillar shape of 40 nm in diameter. The thicknesses of the free and the reference CoFeB layers are 1.7 nm and 1 nm, respectively. The thickness of the MgO layer is 1 nm.

TABLE I. SYSTEM PARAMETERS

Parameter	Value
Gilbert damping, α	0.02
Gyromagnetic ratio, γ	$2.3 \cdot 10^5$ m/(A·s)
Saturation magnetization, M_S	$1.2 \cdot 10^6$ A/m
Free layer thickness, d	1.7 nm
Perpendicular anisotropy energy, K	$9.0 \cdot 10^5$ A/m
Resistance for P state, R_P	14 kΩ
Resistance for AP state, R_{AP}	42 kΩ
Voltage, V	±2 Volts
Switching current for AP→P, $J_{AP\text{->}P}$	$3.8 \cdot 10^{10}$ A/m^2
Switching current for P→AP, $J_{P\text{->}AP}$	$-1.1 \cdot 10^{11}$ A/m^2

With this choice of parameters, the TMR of the structure is 200%, and the thermal stability factor, given by

$$\Delta = \frac{M_S H_K V}{2k_B T}, \quad (8)$$

is equal to 68 at room temperature, in agreement with the minimum factor of 60 required for standalone memories. In (8), H_K is the anisotropy field, V is the volume of the free layer, k_B is the Boltzmann constant and T is the temperature.

Examples of switching realizations in the structure described above are shown in Fig. 3, for both AP→P and P→AP processes. The fluctuating thermal field guarantees a unique switching path every time the simulation is run. Thus, the switching time can vary slightly between different switching realizations. We note that the switching time required to switch from P to AP is higher than from AP to P. This is due to the uncompensated stray field of the reference layer, which tends to keep the magnetization of the two ferromagnets aligned, helping the switching to the parallel configuration and opposing the switching to the antiparallel one. By using a pinned layer antiferromagnetically coupled to the reference layer, we can compensate the total stray field acting on the free layer. This allows to have more symmetric switching times from P to AP and from AP to P, correspondingly.

Fig. 4 reports the switching times (ST) as a function of uncompensated stray field, where the stray field is modeled by the total saturation magnetization of the antiferromagnetically coupled layers. The results are averaged over 30 realizations, in order to take into account the effects of the thermal field. As expected, compensating the stray field results in a higher ST for the AP→P configuration and a lower ST for P→AP. However, results for STs are ~15% higher for AP→P and ~10% lower for P→AP for Model 2 and 3 as compared to Model 1. This

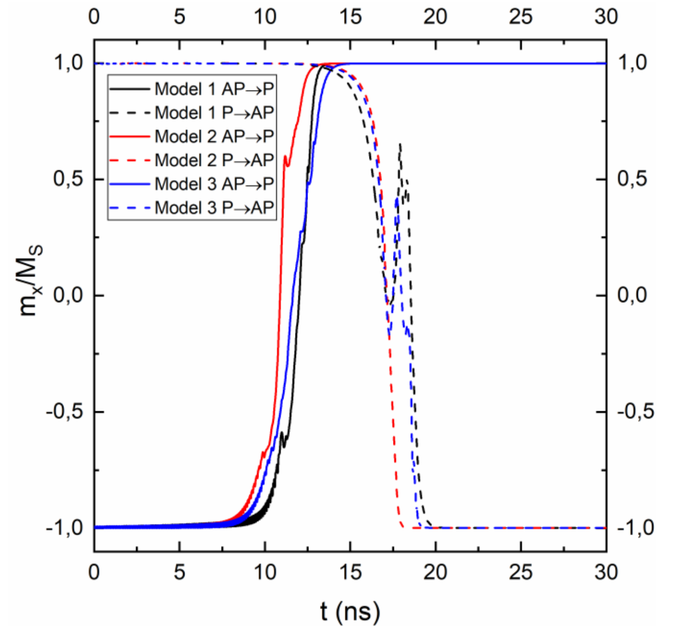

Fig. 3. AP→P and P→AP switching for the 3 different models. In the P→AP switching attempts, the stray field from the fixed layer is opposing the switch, creating the observable oscillations.

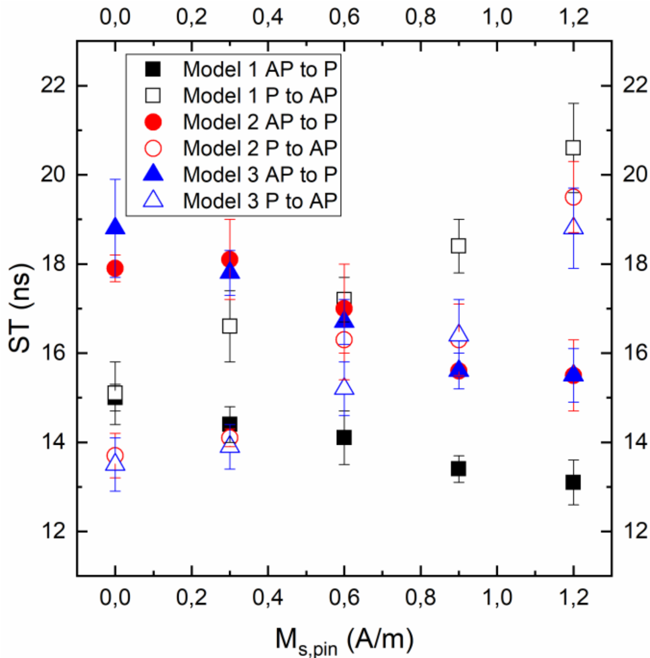

Fig. 4. Comparison between AP→P and P→AP switching for various levels of the uncompensated stray field. Filled symbols represent P→AP switching, empty ones AP→P. The bars show ST variations due to thermal fluctuations for 30 realizations.

discrepancy is attributed to the fact that in Model 1 the *voltage* is fixed, and the total current is allowed to vary according to the MTJ resistance, while Model 2 and 3 are at a fixed total *current* during the whole process.

In order to compensate the effect of the varying resistance on the switching time, we adjust the currents in Model 2 and 3 to make them ~10% higher for AP→P and ~5% lower for P→AP switching. The resulting STs are shown in Fig. 5: with this tuned choice of currents, all the models produce compatible results within the thermal spread. The proposed current adjustment, albeit providing a feasible way of reproducing Model 1 STs distribution using the simplified description offered by (2), depends on the system parameters, especially on the TMR ratio, the dimensions of the stack, and the voltage. Further analysis and simulations are required in order to quantitatively determine the current correction needed to employ the simplified and therefore more computationally efficient model (2) with constant current density.

V. Conclusion

We presented a numerical implementation of the coupled spin and charge drift-diffusion equations for the simulation of magnetization dynamics in a p-MTJ based, high TMR STT-MRAM structure. We compared the results for switching time distribution obtained within the application relevant condition of fixed voltage across the structure to two simplified models of switching under fixed current and fixed current density constraints. The switching times obtained by the three models were compared in the presence of different values of the uncompensated stray magnetic field acting on the free layer. We showed that a TMR and voltage-dependent adjustment of the fixed current values is required for the approximated models to correctly reproduce the switching time distribution in the case of high TMR.

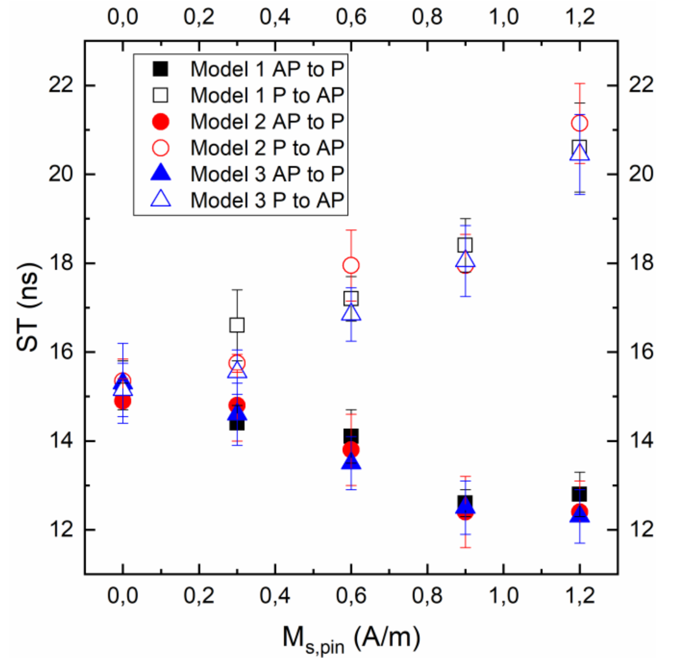

Fig. 5. Comparison of switching times for the tuned values of input currents for models 2 and 3. The switching times of all 3 models are compatible within the thermal spread.

Acknowledgment

This work was supported by the Austrian Federal Ministry for Digital and Economic Affairs and the National Foundation for Research, Technology and Development.

References

[1] D. Apalkov, B. Dieny, J. M. Slaughter, “Magnetoresistive Random Access Memory”, Proc. IEEE 104, 1796 (2016).

[2] O. Golonzka, J. G. Alzate, U. Arslan, M. Bohr, P. Ba *et al*., “MRAM as Embedded Non-Volatile Memory Solution for 22FFL FinFET Technology”, Proc. IEDM 2018, 18.1.1 (2018).

[3] S. Bhatti, R. Sbiaa, A. Hirohata, H. Ohno, S. Fukami *et al*., “Spintronics Based Random Access Memory: a Review”, Mat. Today 20, 530 (2017).

[4] S. Ikeda, J. Hayakawa, Y. Ashizawa, Y. M. Lee, K. Miura *et al*., “Tunnel Magnetoresistance of 604% at 300 K by Suppression of Ta Diffusion in CoFeB/MgO/CoFeB Pseudo-Spin-Valves Annealed at High Temperature”, Appl. Phys. Lett. 93, 082508 (2008).

[5] J.C. Slonczewski, “Current-Driven Excitation of Magnetic Multilayers”, J. Magn. Magn. Mat. 159, L1 (1996).

[6] L. Berger, “Emission of Spin Waves by a Magnetic Multilayer Traversed by a Current”, Phys. Rev. B 54, 9353 (1996).

[7] A. Makarov, “Modeling of Emerging Resistive Switching Based Memory Cells”, Ph.D. thesis, Institute for Microelectronics, TU Wien, Vienna (2014).

[8] J. Slonczewski, “Currents, Torques, and Polarization Factors in Magnetic Tunnel Junctions”, Phys. Rev. B 71, 024411 (2005).

[9] A. Makarov, T. Windbacher, V. Sverdlov, S. Selberherr, “CMOS-Compatible Spintronic Devices: a Review”, Semic. Sci. Tec. 31, 113006 (2016).

[10] D. Aurelio, L. Torres, G. Finocchio, “Magnetization Switching Driven by Spin-Transfer-Torque in High-TMR Magnetic Tunnel Junctions”, J. Magn. Magn. Mat. 321, 3913 (2009).

[11] S. Lepadatu, “Unified Treatment of Spin Torques using a Coupled Magnetisation Dynamics and Three-Dimensional Spin Current Solver”, Sci. Rep. 7, 12937 (2017).

[12] C. Abert, M. Ruggeri, F. Bruckner, C. Vogler, G. Hrkac *et al*., “A Three-Dimensional Spin-Diffusion Model for Micromagnetics”, Sci. Rep. 5, 14855 (2015).

[13] S. Ikeda, K. Miura, H. Yamamoto, K. Mizunuma, H. D. Gan *et al*., “A Perpendicular-Anisotropy CoFeB-MgO Magnetic Tunnel Junction”, Nat. Mater. 9, 721 (2010).